# GaAs X- Ray System Detectors for Medical Applications

MARIA RIZZI, MICHELE MAURANTONIO, BENIAMINO CASTAGNOLO

Dipartimento di Elettrotecnica ed Elettronica,
Politecnico di Bari
v. E. Orabona, 4 - 70125 Bari
ITALY

*Abstract*: In this paper we discuss some modeling, simulation, implementation and test issues, with respect to the development of the GaAs system detector based on a microstrip configuration for medical application. The chosen strip architecture has simple electrodes structure and low channel-capacitance. Different basic strip schemes have been proposed and devised. To reduce the coupling between strip, a structure in which every strip-detector is surrounded by guard-ring has been considered and the performance has been evaluated. Detector fabrication has been completed and test phase is now under way: to this purpose a suitable test environment has been devised and test strategies have been planned.

*Key words:* X-ray detector, GaAs, microstrips, Schottky diode

## 1 Introduction

The main advantages of digital sensors compared to the photographic film are higher sensitivity, better linearity and dynamic range. Behavioral specifications of particle detectors may significantly differ from conventional imaging applications: higher spatial resolution is desired in this case and sparse radiation events over relatively large surfaces are to be covered. Hybrid (strips detectors) as well as monolithic detectors have been developed for different field such as medical and high energy applications. In the field of X-ray detection, many materials have been studied to create detectors. In particular Cadmium Telluride (CdTe) and Gallium Arsenide (GaAs) have been adopted to realize high efficiency X-ray detectors, owing to their large atomic number and value of the forbidden gap. Detector performance is affected not only by the chosen semiconductor but also by the adopted architecture. GaAs is a very good candidate for the detection of low energy X-rays at room temperature, thanks to its high Z-value, with consequent high detection efficiency and important reduction of the dose to the patient [I]. In this paper, a brief description of a model which has been developed to be used in the synthesis of a GaAs microstrip detector. In section 2 the principles of the simulation method used to determine the photo-generation current is presented. In section 3, the GaAs detection property and some fabrication options are indicated. In section 4 the detector is characterized through the comparison with the modeling data. In section 5, to evaluate the behavior of the system, the electrical characterization has been performed considering different detectors and adopting some optimization arrangements to reduce coupling phenomena. In particular, performance of different insulated strip structures is evaluated and characteristics of the whole detector are studied. Finally, some conclusions are drawn out

## 2 Mathematical model

To link the characteristics of the X-ray system detector with the device performance, a 3D numerical model of the photo-effect generated current has been studied [2]. The model adopts the Finite Element Method analysis and is implemented in Matlab 7.01 R14 environment.

This model evaluates the current signal induced by the motion of a single photo-generated carrier by the Ramo's theorem [3], [4].

When a carrier pair is generated in a given position, the charge induced on the collecting electrode is calculated taking into account the contribution of both electrons and holes. If trapping occurs, an incomplete charge collection is observed[5][6][7]. The Shockley-Read-Hall (SRH) recombination theory is considered as basic model for the carriers trapping and generation phenomena. Supposing that $\delta n_0$ electron/hole pairs are generated at initial time at a generic $P_0$ ($x_0$,$y_0$,$z_0$) point between the Schottky contacts, the charge induced by the motion of electrons and holes, before reaching the electrodes, is:

$$\Delta Q_{e/h}(t) = \pm \delta n_0(t) q \frac{(x(t) - x_0)}{D}.$$

Here electrons are supposed to move along the positive x direction and holes in the opposite direction.
Considering separately the effect of electrons and holes, the expression of the total charge induced is [8]:

$$\Delta Q^0{}_{tot} = \Delta Q^0{}_e + \Delta Q^0{}_h \quad (9)$$

where

$$\Delta Q^0{}_e = \frac{q}{D} \sum_{i=i_0}^{i_D} \delta N_0(t_i, x_i)\, \Delta x_i \quad (10)$$

$$\Delta Q^0{}_h = \frac{q}{D} \sum_{i=0}^{i_0} \delta N_0(t_i, x_i)\, \Delta x_i \quad (11).$$

The electron current signal at the i-th iteration step, can be approximated as follows:

$$I_e(t_i) = \frac{\Delta Q^0{}_e(t_i) - \Delta Q^0{}_e(t_{i-1})}{\Delta t_i}$$

and a similar expression is valid for the hole current $I_h(t_i)$.
The same mathematical procedure can be iterated for every generation point. Therefore, it is possible to evaluate the overall collected charge by summing contributions from all the generation points. This model, validated for a singe pixel [2], is now applied to strip structure.

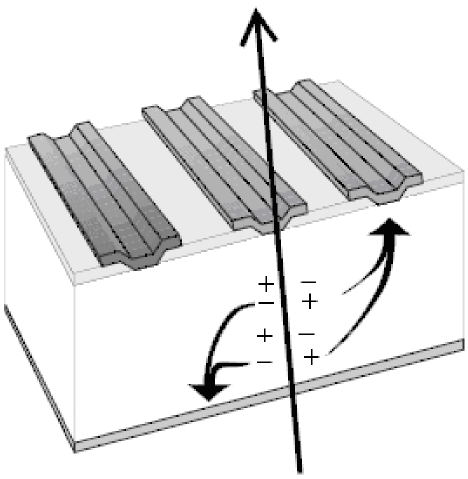


Fig 1 Electron-hole photo-generation phenomena on a microstrip structure

## 3 GaAs Detector Realization

The distribution of defects found in a given sample of GaAs depends on the growth method [9]. Detectors samples witch have been realized for study purpose are made on semi-insulating, Vertical Gradient Freeze (VGF), (100) oriented, single crystal GaAs substrates, 200, 600 and 1000μm thick. The substrate has resistivity of $9.3 \times 10^7 \Omega$cm, mobility equal to $6944 cm^2 V^{-1} s^{-1}$, carriers concentration of $9.4 \times 10^6$ $cm^{-3}$ and the Etch-Pith-Density (EPD crystal defect) of 1055 $cm^{-2}$.
Each detector consists of two Schottky junctions, one of which inversely biased (fig.2). They are connected to an electronic front-end which provides for recording and amplifying signals. The Schottky contacts were realized on the front and on the back surfaces of the wafer with Ti/Pt/Au metallization process [10]. The behavior of several strips surrounded by a guard-ring has been studied (fig. 2).

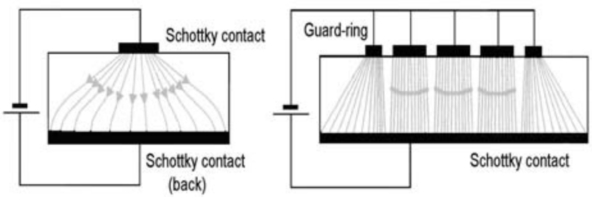


Fig.2 J flux lines distribution

The main reason for the presence of a guard-ring is that it limits the surface leakage current and corrects the electric field under the outer strip in the array. In fact, due to the border effects, they could have a different behavior, in particular regarding the energy resolution (ΔE/E) and the charge collection efficiency (CCE).
A set of lithographic masks was designed. A first mask for the deposition of metal contacts, a second mask for the realization of passivation and insulating layers and a third mask for the implementation of micro-contact pads.
The realized detector (figs. 3a-3b) has a strip structure with all the combinations of the following parameters

- Strip width: 20, 30, 40, 50 μm
- Inter-strip distance: 5, 10, 20, 30 μm

The single strip is Schottky contacts made of a Ti/Pd/Au multilayer deposited by an electron beam system at pressure of $10^{-7}$ mbar.

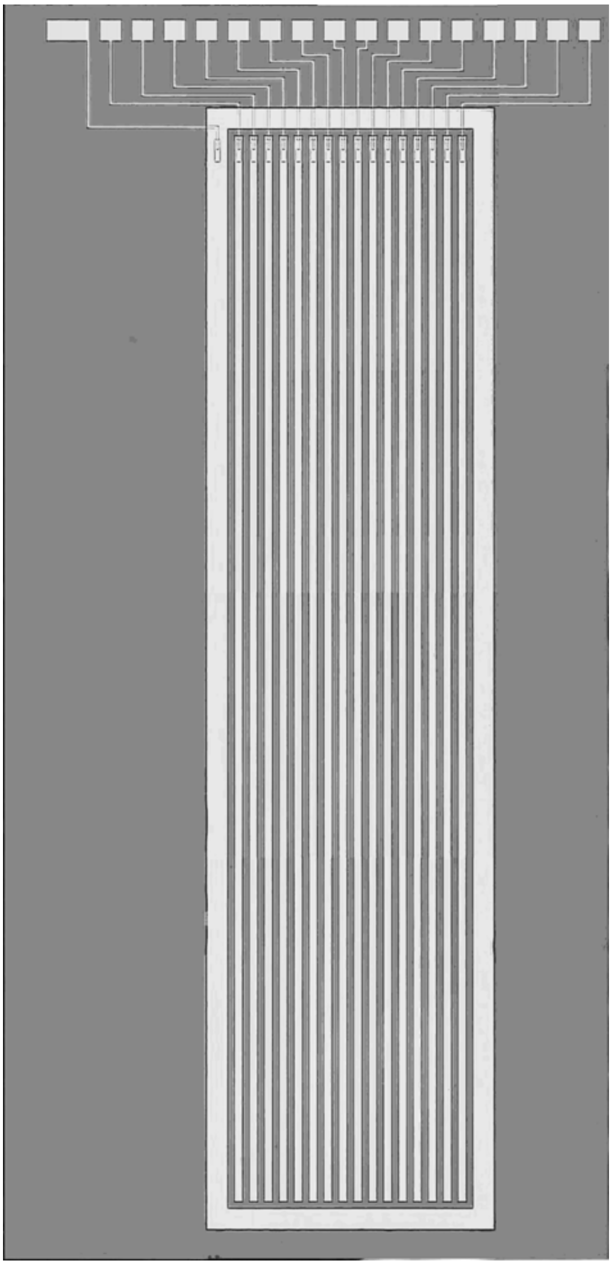

Fig 3a Microphotography of a detector with strips length 50 μm

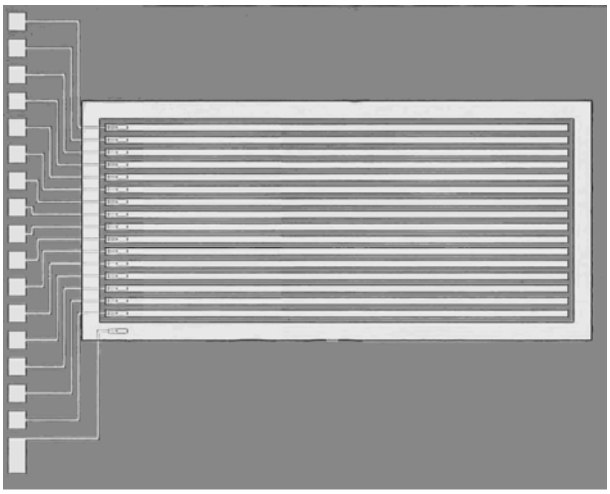

Fig 3b Microphotography of a detector with strips length 20 μm

The guard-ring is placed at a distance equal to the inter-strip distance (fig. 4).
The thickness of the Ti/Pd/Au multilayer is 300Å/300Å/600Å.
The analysis of the structure was carried out employing laser pulses having a temporal width lower than the charge collection time.
Two different laser sources were used: a pulsed laser diode Hamamatsu PLP-02 and a mode-locked Nd-glass laser with an optical parametric oscillator having a pulse width of 20ps.

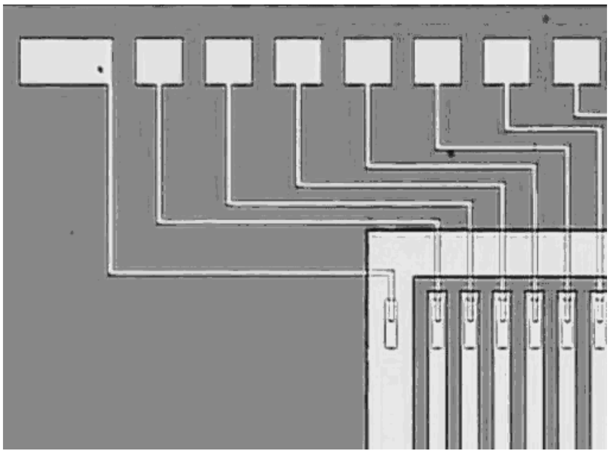

Fig 4 Particular of strip detector's guard ring

## 4 Electrical characterization

To characterize the detector, the static current-voltage (I-V) and capacitance-voltage (C-V) curves have been drawn. The obtained results are indicated in fig. 7 and fig. 8 for a detector having an inter-strip distance equal to 10μm, length equal to 50μm and substrate thickness (T) of 200μm (fig. 3a).
The shapes in figures 7 and 8 indicate a weak coupling between strips and between strips and guard-ring. In fact the external strip have higher capacitance values than the inner ones.

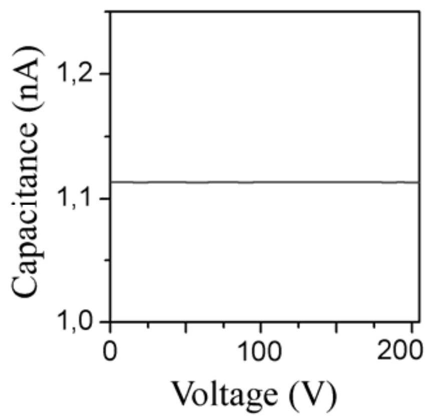


Fig 7 Strip-back capacitance values for the central strip

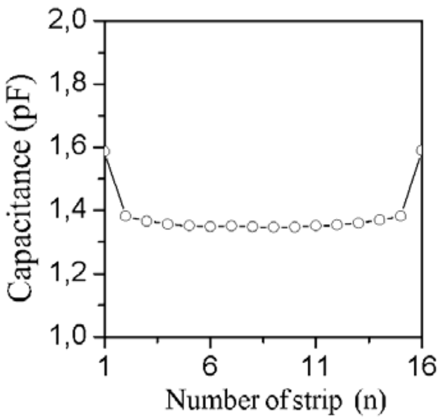

Fig 8 Strip-back capacitance values for strips having different positions

To confirm the coupling phenomena, the comparison of the capacitance values calculated adopting the expression C=εA/S with those experimentally measured, is shown.
For example, considering a detector 200μm thick, the measured value is 1,8pF while the geometrical value is 1.5pF.
Figure 9 and figure 10 shows that the measured capacitance values approximate the geometrical values as T and W increases.

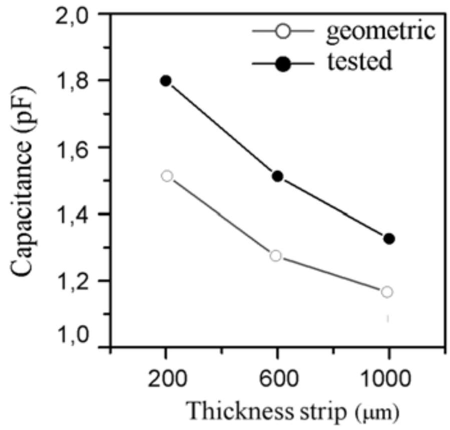

Fig 9 Strip-back capacitance values for strips having different substrate thickness.

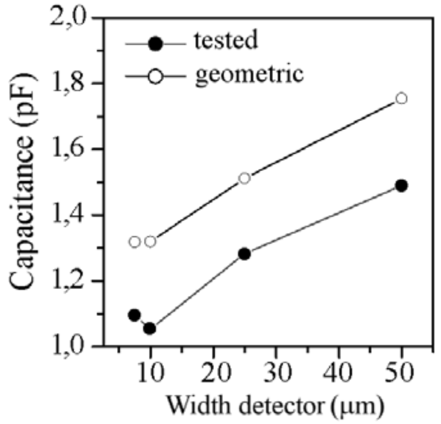

Fig 10 Strip-back capacitance values for a detector having different inter-strip distance.

From table 1 it is evident that increasing the strip width, the electrical field lines tend to be normal to the detector surface. Moreover, the capacitance value is almost independent of the inter-strip distance and the inter-strip capacitance is unrelated to the analyzed strip couple (table 2)

| W (μm) | L (μm) | $C_{test}$ (pF) | $C_{geom}$ (pF) | $C_{test}/C_{geom}$ |
|---|---|---|---|---|
| 30 | 40 | 1.13 | 0.03 | 34 |
| 100 | 40 | 1.12 | 0.03 | 33.6 |
| 30 | 200 | 1.95 | 0.5 | 3.9 |
| 100 | 200 | 1.80 | 0.5 | 3.6 |

Table 1 Results of tested capacitance, theorical geometric capacitance, their relationship for different width W and length L. The thickness of detectors is 200 μm

| | $C_{inter-string}$ (pF) | | $C_{strip-g. ring}$ (pF) |
|---|---|---|---|
| 1 - 2 | 0.33 | 1 – g.ring | 0.41 |
| 8 - 9 | 0.34 | 8 – g.ring | 0.08 |
| 15 - 16 | 0.34 | 16– g.ring | 0.41 |

Tab 2 Results of tested capacitance between strips and between strips and guard-ring, for detector with W=30 μm, L=50 μm and T=200 μm.

## 5 Detector performance

To characterize in dc detectors, a five micro pointed probe was used. The micropoints were connected to the back, to the guard-ring and to three adjacent strips respectively. The I/V curve was obtained applying a variable voltage (0-200V) to the back electrode and grounding the guard-ring and the strips (fig.12).

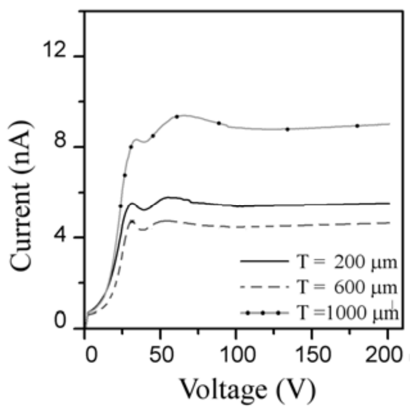

Fig 12 I/V shape for back, guard ring and strip

Fig.13 show the I/V characteristic for two different inter-strip values, considering a 10μm

inter-strips distance. In fig.14 and 15 the shape of the strip current curve is plotted considering the same value of width, T and length as parameters.
For low voltage values, the different curves have similar trends while for higher values shapes differ. Depending upon the results of figs. 14 and 15, current increases as the electrode area on the detector widens.

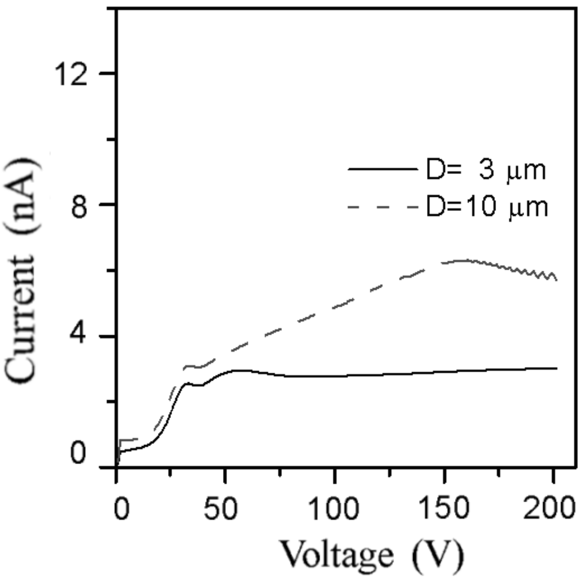

Fig 13 $I_{strip}$ for two different inter-strip (D) values with the same values L and T

It is important to underline that breakdown events never occurred in all measures in the considered voltage range (0-200V).

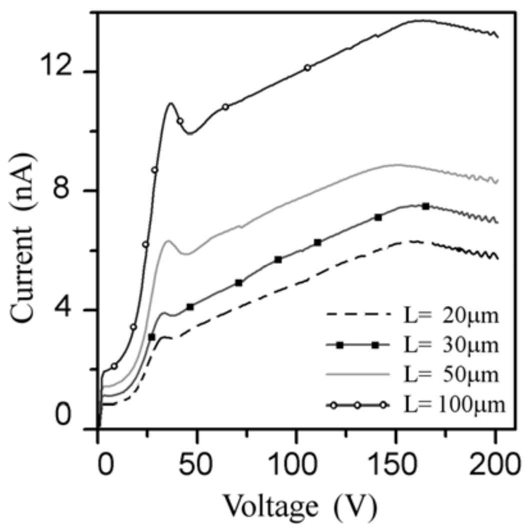

Fig 14 $I_{strip}$ for different Length values with the same values W and T

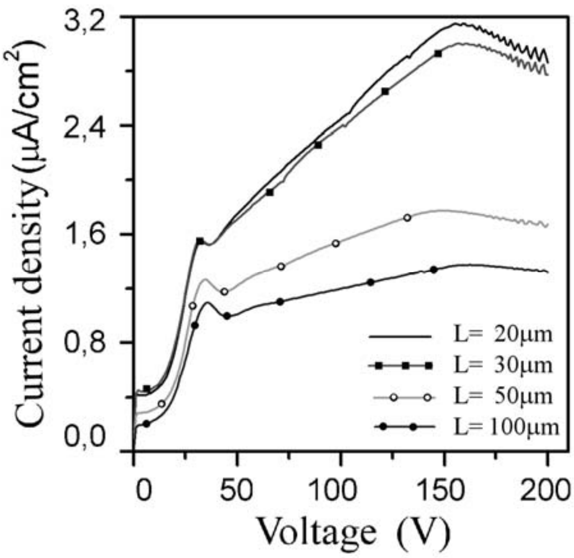

Fig 15 $J_{strip}$ for different Length values with the same values W and T

## 6 Conclusions

In this paper the behavior of different microstrip detector systems, made of high quality SI-VGF GaAs detectors was investigated. Good performance was obtained at room temperature operation.
The agreement between measurements and simulations, made taking into account also the influence of geometrical effects, such as different widths and thicknesses, is satisfactory.
This type of detector system has many advantages:

- one-dimensional position sensitivity with single-sided processing;
- small number of readout channels;
- no bump-boding required to connect the strips;
- different sets of strips (i.e. X- and Y-strip) can use identical readout electronics;
- it is possible to use stereo angles (0< α <90) between the two strip sets, or add more channels (i.e. a third set of strips) to partially solve the multi-hit ambiguity problem.

It is clear that, for small scale applications, such as in cases where micron and sub-micron 1-D resolutions are required, or in the cases were strip pitch and length are not too large, strips detectors cannot be used. However, for almost all other situations, strip detectors can be applied favorably for their low cost of fabrication.
This system, finally, is a good candidate for medical applications because it allows a satisfactory detection efficiency in the energy

range typical of mammography, radiography and nuclear medicine (15-100 keV).

*References*


[I] R. Bertin, S. D'Auria, C. Del Papa, F. Fiori, B. Lisowski, V. O'Shea, P. G. Pelfer, K. Smith, A. Zichichi, “A preliminary study of GaAs solid-state detectors for high-energy physics” *Nuclear Instruments and Methods in Physics Research Section A,* vol. 294, issues 1-2, pp. 211-218, 1990

[2] M. Rizzi, M. Maurantonio, B. Castagnolo “3D-Finite Element Model for GaAs α-particles pixel detector” *proceedings of 4th WSEAS International Conference on ELECTRONICS, HARDWARE, WIRELESS and OPTICAL COMMUNICATIONS (EHAC 2005),* Salzburg, AUSTRIA, February 13-15, 2005

[3] P. De Visschere “The validity of Ramo’s Theorem” Solid State Electronics, vol.4, pp.455-459, 1990

[4] H. Kim, H.S. MIN, W. Tang, Y.J. Park “An extended proof of the Ramo-Shockley theorem“, *Solid State Electronics*, vol.34, pp.1251-1253, 1991

[5] A.Cola, F.Quaranta, L.Vasanelli, C.Canali, A.Cavallini, F.Nava, and M.E.Fantacci, “A Study of the Trap Influence on the Performances of Semi-Insulating GaAs Pixel Detectors” *Nuclear Instruments and Methods in Physics Research,* pp. 395 349, 1997

[6] A. Cola, F. Quaranta, M.A. Ciocci, M.E. Fantacci, "A Study of the Electrical and Charge Collection Properties of Semi-Insulating GaAs Detectors", *Nuclear Instruments and Methods*, Vol. A380, pp. 66-69, 1996

[7] S: P. Beaumont, F. Foster, G. Hughes, B. K. Jones, J. Santana I. J. Saunders, T. Sloan, "GaAs solid state detectors for particle physics", *Nuclear Instruments and Methods in Physics Research*, A322, 472-482, 1992

[8] M. Rizzi, V.Antonicelli, B. Castagnolo, “New model for a GaAs X-ray pixel detector” *IEE Proceedings on Circuits, Devices and Systems*, vol. 150 ,n. 3 , 6 pp. 210–216, 2003

[9] D. S. McGregor, D. A. Rojeski, "Evidence for field enhanced electron capture by EL2 centers in semi-insulating GaAs and the effect on GaAs radiation detectors", Journal of Applied Physics, Vol. 75 N. 12, p. 7910, 1994

[10]B. L. Sharma “Metal-semiconductor Schottky barrier junction and their applications”, *Plenium Press,* 1994



**Acknowledgement**

The work is carried out under the financial support of the Ministero dell'Istruzione, dell'Università e della Ricerca Scientifica, in the frame of Cluster C26: "*Modellazione, sperimentazione e diagnostica di strutture in materiali innovativi*".

Thanks are due to Consortium OPTEL (Brindisi - Italy) for the kind help in processing the detectors.